

Optical signatures of strain-induced ferromagnetism in LaCoO₃ thin film

F. Abadizaman,¹ M. Kiaba,¹ and A. Dubroka^{1,2,*}

¹*Department of Condensed Matter Physics, Faculty of Science,
Masaryk University, Kotlářská 2, 611 37 Brno, Czech Republic*

²*Central European Institute of Technology, Brno University of Technology, 612 00 Brno, Czech Republic*

(Dated: April 17, 2024)

Using spectroscopic ellipsometry, we studied the optical conductivity of LaCoO₃ with various degrees of strain. The optical response of the compressively strained LaCoO₃ film is qualitatively similar to the one of the unstrained LaCoO₃ polycrystalline sample and exhibits redistribution of the spectral weight between about 0.2 and 6 eV, which is most likely related to the thermal excitation of the high-spin states. The optical response of the ferromagnetic tensile strained film exhibits clear signatures due to the ferromagnetic state. Below the Curie temperature $T_c = 82$ K, the spectral weight is transferred with the increasing temperature from low energies between 0.2 and 3.3 eV to energies between 3.3 and 5.6 eV. The temperature dependence of the low-energy spectral weight between 0.2 and 3.3 eV can be understood in the framework of the high-spin biexciton model of Sotnikov and Kuneš as corresponding to the variation of the concentration of high-spin states that are stabilized below T_c . The magnitude of redistribution of spectral weight due to the formation of the ferromagnetic state is sizable. We estimate that it corresponds to a lowering of the kinetic energy of 13 meV per Co ion, which is about two times $k_B T_c$. The latter shows that the saving of the kinetic energy is important and may be the leading energy contribution in the formation of the ferromagnetic phase.

I. INTRODUCTION

LaCoO₃ has been studied extensively for its unusual magnetic and electronic properties. At low temperatures below 50 K, bulk LaCoO₃ exhibits a nonmagnetic insulating behavior with a small optical gap of about 0.2 eV [1, 2]. In an intermediate temperature range between about 50 – 400 K, it exhibits paramagnetic properties while preserving the insulator properties with a reduced resistance compared to the low-temperature values [1]. At temperatures above 500 K, the insulator-to-metal transition occurs [1]. The magnetic properties of LaCoO₃ can be altered by strain. It was observed that the tensile strain induces ferromagnetic (FM) order while LaCoO₃ remains insulating [3]. The microscopic mechanism of this FM state is likely qualitatively different from the double-exchange mechanism of the FM state occurring in conducting doped cobaltites [4, 5], and its nature is a topic of an ongoing debate [6–10].

The unusual electronic and magnetic properties of bulk LaCoO₃ are caused by the specific electronic structure where several spin states are nearly degenerate. It is generally accepted that the unusual behavior at the intermediate temperature range is caused by thermal excitation of higher spin states compared to the low-temperature low-spin (LS) ground state, with the Co electronic configuration t_{2g}^6 . There has been a long debate over which spin state is excited at higher temperatures, whether these are dominantly intermediate-spin (IS) states, $t_{2g}^5 e_g^1$, or high-spin (HS) states, $t_{2g}^4 e_g^2$ [11–20]. This debate was recently advanced by a joint theoretical and experimental work

reporting a pronounced dispersion of IS excitations [21–23]. This led to a model of thermally excited HS excitons viewed as a biexciton consisting of tightly bound (on the same Co atom) IS excitons with different orbital character. In this approach, both IS and HS states are essential in the understanding of the low-energy dynamics of LaCoO₃. The energy of HS biexciton is about 20 meV at low temperatures, and its energy significantly increases with temperature [23].

The strain-induced FM state in LaCoO₃ is usually induced by a substrate with a small lattice mismatch in epitaxial films. The Curie temperature (T_c) of LaCoO₃ films deposited on (100) oriented LSAT or SrTiO₃ substrates is about 80–85 K [8, 24–28] and the T_c can reach up to 94 K in films deposited on (110) oriented LSAT substrates [6]. Several aspects potentially important for the mechanism of the FM state were reported. Lattice distortion with propagation vector (1/4,-1/4,1/4) was observed [6], an important role of the oxygen vacancies was suggested [7, 8] and microscopic inhomogeneities of the FM state were observed [9]. Recently, in the framework of HS biexciton model [23], it was proposed by Sotnikov and Kuneš that the strain-induced ferromagnetism originates from the interaction between HS states via virtual IS states [10].

In this paper, we would like to contribute to the discussion about the mechanism of the strained induced FM state by examining its optical response. We study the optical properties of unstrained LaCoO₃ (polycrystalline sample) and tensile and compressively strained LaCoO₃ films using ellipsometry in the energy range of the interband transitions between 0.2 and 6.5 eV. Ellipsometry is an established technique that allows the determination of the optical response with a high sensitivity and reproducibility. The temperature-dependent opti-

* dubroka@physics.muni.cz

cal response in a wide energy range allows to map the essential redistribution of electronic spectral weight due to the electronic/magnetic transitions, which reflects the changes in the underlying electronic structure [29]. We observed that the compressive strain does not qualitatively change the optical response. In contrast, in the FM tensile strained film, the optical response is significantly altered and exhibits clear signatures due to the formation of the FM state. We determine the energy range of the FM-related redistribution of the spectral weight and quantify its magnitude.

II. EXPERIMENT

In this report, LaCoO₃ samples with different degrees of strain were studied: polycrystalline LaCoO₃ (no strain), LaCoO₃ thin film deposited on LaAlO₃ substrate (compressive strain) and LaCoO₃ thin film deposited on (LaAlO₃)_{0.3}(Sr₂TaAlO₆)_{0.7} (LSAT) substrate (tensile strain). The thin films were grown using pulsed laser deposition and annealed *in situ* at the deposition temperature of 650 °C under 10 Torr oxygen pressure to decrease oxygen vacancy concentration [30]. The lateral dimension of thin films is 10×10 mm², and the thickness of the films was determined using X-ray reflectivity (Rigaku Smartlab) to be about 22 nm. Ellipsometry measurements were performed on the samples and the bare substrates with Woollam VASE ellipsometer (0.6 - 6.5 eV) and Woollam IR-VASE ellipsometer (0.1 - 0.6 eV) in the temperature range from 300 to 7 K. The measurements were repeated several times and were found reproducible. The optical constants of the thin film were obtained at each measured energy from the ellipsometric angles Ψ and Δ using the standard model of coherent interferences in a thin film on a substrate [31] without the involvement of the Kramers-Kronig relations. The measurements of the magnetic moment were performed using a vibrating sample magnetometer (Quantum Design Versalab).

III. DATA ANALYSIS AND DISCUSSION

We have probed the structural properties of our films using X-ray diffraction. The reciprocal space maps of the LaCoO₃ film deposited on LSAT substrate (LaCoO₃/LSAT) measured near the symmetrical (004) diffraction and near the asymmetrical (103) diffraction are shown in Fig. 1(a) and (b), respectively. Analogical maps for the LaCoO₃ film deposited on LaAlO₃ substrate (LaCoO₃/LaAlO₃) are shown in Fig. 1(c) and (d). They exhibit strong maxima due to the substrate diffraction and distinct maxima due to the LaCoO₃ diffraction at the same Q_z values, depicting that the films are epitaxial and fully strained. The lattice parameters of the samples were determined from the positions of the LaCoO₃ diffractions, and the results are shown in Table I, including the

in-plane and out-of-plane values of film strain obtained from the lattice constants. The LaCoO₃/LSAT film has a tensile strain of 1.07 %, whereas the LaCoO₃/LaAlO₃ film exhibits a compressive strain of -0.99 %.

Figure 2(a) shows the temperature dependence of magnetization of all samples measured in a magnetic field of 10 mT parallel to their surface. The LaCoO₃/LSAT film exhibits an onset of FM phase with T_c of about 82 K, whereas the other samples are non-magnetic in the measured temperature range. The value of the saturated magnetic moment of the LaCoO₃/LSAT film at 50 K is obtained from the hysteresis loop shown in Fig. 2(b) and amounts to $\mu_s = 0.5 \mu_B/\text{Co}$ which is in a good agreement with Refs. [27] and [28].

An overview of the optical data is presented in Fig. 3. The left, middle, and right column corresponds to the LaCoO₃ polycrystal, the LaCoO₃/LaAlO₃ film, and the LaCoO₃/LSAT film, respectively. The top row presents the real part of the optical conductivity $\sigma_1(E)$ as a function of energy E of the incident photons. Overall, the spectra of all samples have similar shapes. They exhibit an optical gap between 0.2 to 0.3 eV and several inter-band transitions at higher energies that were interpreted as due to Co $t_{2g} \rightarrow t_{2g}$ transitions (centered at 0.5 eV), Co $t_{2g} \rightarrow e_g$ transitions (centered at 1.5 eV) and O $2p \rightarrow \text{Co } e_g$ transitions (centered at 3 eV) [2], as marked in Fig. 3(a) by arrows. There is additionally a band near 5.8 eV that corresponds to transitions involving La orbitals since its intensity decreases with increasing Sr doping in La_{1-x}Sr_xCoO₃ [5].

The optical data of strongly correlated electronic materials are often discussed in terms of the effective concentration of charge carriers (or spectral weight) that is a measure of absorption of the electromagnetic radiation in an energy interval ($\hbar\omega_L$, $\hbar\omega_H$):

$$N_{\text{eff}}(\omega_L, \omega_H) = \frac{2mV}{\pi e^2} \int_{\omega_L}^{\omega_H} \sigma_1(\omega) d\omega, \quad (1)$$

where m is the electron mass, V is the volume of the unit cell, and e is the elementary charge [29]. The amount of the spectral weight and the energy intervals where it is

TABLE I. Lattice parameters of samples determined by X-ray diffraction. For the bulk samples (polycrystalline LaCoO₃ and the substrates), the lattice parameter corresponds to the bulk pseudocubic lattice constant whereas for the films, it denotes the out-of-plane lattice constant.

Sample	lattice constant (Å)	ε_{\perp} (%)	ε_{\parallel} (%)
polycrystalline LaCoO ₃	3.825		
LaAlO ₃ substrate	3.787		
LSAT substrate	3.866		
LaCoO ₃ /LaAlO ₃ film	3.853	0.73	-0.99
LaCoO ₃ /LSAT film	3.792	-0.86	1.07

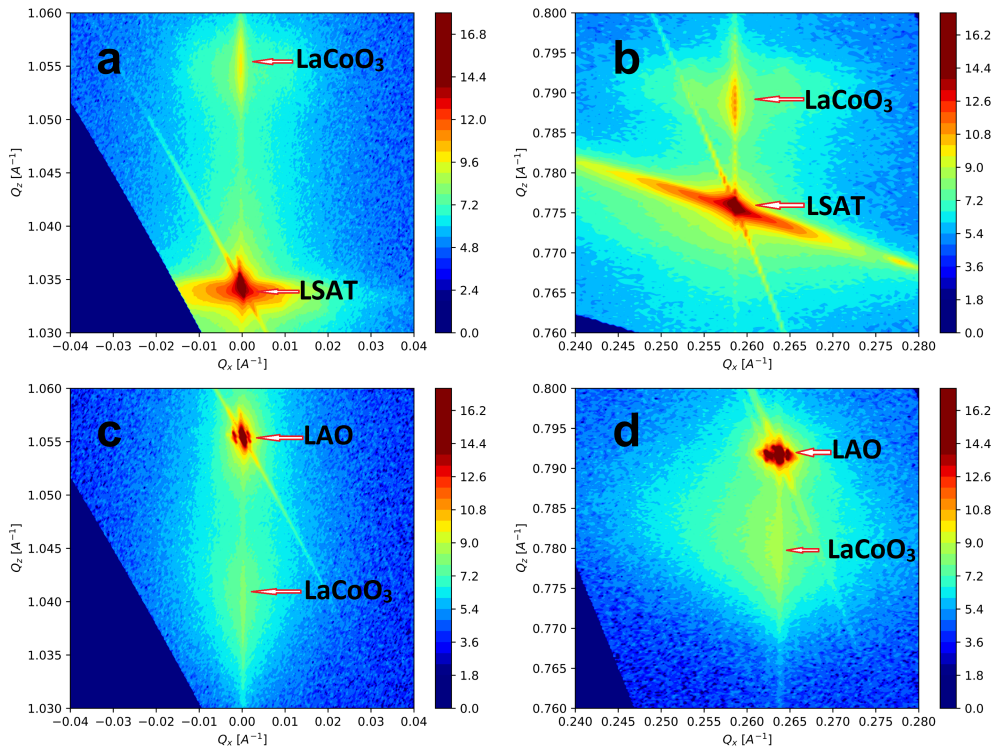


FIG. 1. X-ray reciprocal space maps of LaCoO_3 film grown on LSAT substrate near the symmetrical (004) diffraction (a) and near the asymmetrical (103) diffraction (b). The diffractions due to the substrate and LaCoO_3 are denoted by the arrows. Analogical maps are shown for the LaCoO_3 film grown on LaAlO_3 (LAO) substrate in panels (c) and (d).

redistributed are often evaluated because they reflect the underlying electronic structure and correlations. We recall that the optical sum rule states that the total spectral weight $N_{\text{eff}}(0, \infty)$ is equal to the total concentration of charge in a sample, and, consequently, it is temperature independent apart from the effects of thermal expansion that are usually very small and can be neglected.

To visualize the redistribution of spectral weight with temperature, the second row of Fig. 3 shows the real part of the optical conductivities relative to the one measured at the lowest temperature of 7 K, $\sigma_1(T) - \sigma_1(7 \text{ K})$. Figure 3(d) presents the relative conductivity of LaCoO_3 polycrystalline and depicts that there are several so-called isosbestic energies (energies where the conductivity is essentially temperature-independent) that we denote E' , E_M and E_H . The largest changes of the spectral weight with increasing temperature involve a decrease between the energies $E_M = 3.4 \text{ eV}$ and $E_H = 6.2 \text{ eV}$ and an increase at lower energies between $E_g = 0.2 \text{ eV}$ and $E' = 1.9 \text{ eV}$. Additionally, there is a smaller temperature dependence of conductivity between E' and E_M . In the view of the sum rule, we can interpret these findings as a transfer of spectral weight with increasing temperature from high energies between E_M and E_H to lower energies between E_g and E_M . Similar redistribution of optical spectral weight in bulk LaCoO_3 was previously observed by Tokura *et al.*[1] where it was reported that with in-

creasing temperature, the low-energy spectral weight below 1.4 eV increases on the expense of spectral weight at higher energies. Note that a similar redistribution of the spectral weight induced by a laser pulse was observed with femtosecond ellipsometry [32]. The reported crossing point was found to be about 2.1 eV, close to the $E' = 1.9 \text{ eV}$ found in this report. In the context of the HS biexciton model [23], the observed redistribution of spectral weight is most likely related to the thermal excitation of the high-spin biexcitons and corresponding changes in the occupation of t_{2g} and e_g orbitals.

The relative conductivity of the compressively strained $\text{LaCoO}_3/\text{LaAlO}_3$ film is shown in Fig. 3(e). Qualitatively, the spectra are similar to those of the polycrystalline LaCoO_3 shown in Fig. 3(d) with slightly different values of the characteristic energies $E' = 1.7$, $E_M = 3.6$ and $E_H = 5.9 \text{ eV}$ and overall larger magnitude of the changes. Particularly, the spectra exhibit the same redistribution of spectral weight with increasing temperature from high energies between E_M and E_H to lower energies between E_g and E' .

The third row of Fig. 3 displays the relative effective concentration of charge carriers with respect to 7 K, $\Delta N_{\text{eff}}(E) = N_{\text{eff}}(0.1 \text{ eV}, E, T) - N_{\text{eff}}(0.1 \text{ eV}, E, T = 7 \text{ K})$, as a function of the high-energy cut-off $E = \hbar\omega_H$. The low energy cut-off was chosen to be $\hbar\omega_L = 0.1 \text{ eV}$, right below the optical gap. There is thus a small miss-

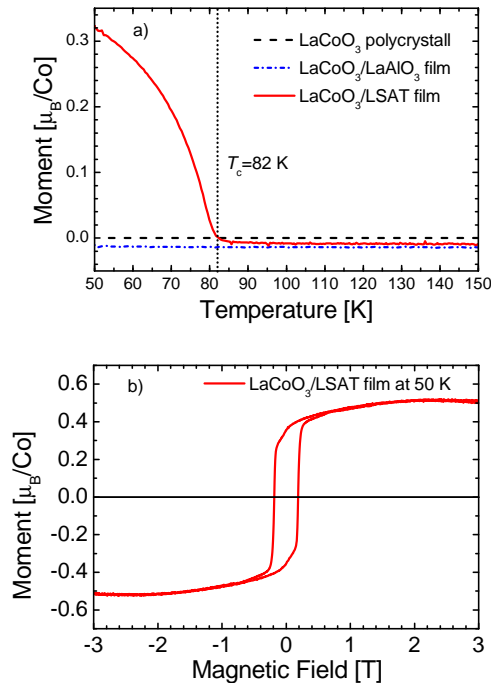


FIG. 2. a) Magnetic moment as a function of temperature of LaCoO₃ polycrystalline sample and the LaCoO₃/LaAlO₃ and LaCoO₃/LSAT films, measured in a magnetic field of 10 mT. b) Hysteresis loop of the LaCoO₃/LSAT film acquired at 50 K.

ing spectral weight due to phonons, but it is negligible compared to the spectral weight of the interband transitions. The intersection of $\Delta N_{\text{eff}}(E)$ with zero denotes the energy below which the redistributions of spectral weight are compensated. For the polycrystalline LaCoO₃ and for the temperature of 220 K, such a zero crossing occurs near $E^* = 5.1$ eV, see Fig. 3(g), and for the compressively strained LaCoO₃, it occurs near $E^* = 5.3$ eV, see Fig. 3(h). These values of E^* indicate that the spectral weight of the pronounced dip near 5.8 eV in Figs. 3(d) and (e) is not transferred with decreasing temperature to lower energies but to energies above E_H .

The qualitative similarity between the unstrained polycrystalline LaCoO₃ and the compressively strained LaCoO₃/LaAlO₃ film can also be seen in the temperature dependence of the low-energy spectral weight $N_{\text{eff}}(E_g, E')$ shown for LaCoO₃ polycrystal in Fig. 3(j) and for LaCoO₃/LaAlO₃ film in Fig. 3(k). Both exhibit a monotonically increasing trend with temperature, which likely corresponds to the thermal population of HS states. The similarity of the redistribution of the spectral weight between unstrained polycrystalline LaCoO₃ and the compressively strained LaCoO₃/LaAlO₃ film indicates that the compressive strain does not induce a significant modification of the electronic structure of LaCoO₃. The only significant difference is quantitative — the changes with

temperature in the compressively strained LaCoO₃ are about twice larger than those of the unstrained LaCoO₃. This likely corresponds to a lower activation energy of the HS states in compressively strained LaCoO₃ compared to the unstrained LaCoO₃.

Figure 3(f) displays the relative conductivity of the FM LaCoO₃/LSAT film. Apparently, the temperature dependence shows qualitative differences with respect to the previous cases shown in Fig. 3(d) and (e). For example, the isosbestic point near the middle of the measured range at $E_M = 3.3$ eV has the opposite signature, i.e., the conductivity with increasing temperature decreases below E_M in contrast to Fig. 3(d). The origin of the differences becomes clear from the temperature dependence of the low energy spectral weight $N_{\text{eff}}(E_g, E_M)$ shown in Fig. 3(l), which exhibits a clear onset at T_c with the square root behavior typical for the temperature dependence of an order parameter of a second order phase transition. The optical response exhibits clear signatures due to the formation of the FM phase.

Figure 4(a) displays in detail temperature dependence of the relative optical conductivity $\sigma_1(T) - \sigma_1(7\text{ K})$ of the LaCoO₃/LSAT film only below and near T_c . Since in this temperature range, the temperature changes due to non-magnetic processes are weak, the majority of conductivity changes correspond to the formation of the FM phase. The spectra exhibit isosbestic points $E_M = 3.3$ eV and $E_H^{\text{FM}} = 5.6$ eV as denoted by the arrows. The temperature dependence forms a butterfly-like shape with the isosbestic point E_M in the center with two “wings” with roughly a similar area between $E_g - E_M$ and $E_M - E_H^{\text{FM}}$. The spectral weight is transferred with increasing temperature from the low-energy wing into the high-energy wing; therefore, the spectral weight redistribution has the opposite trend to the one observed in the unstrained LaCoO₃ shown in Fig. 3(d). Note, however, that the redistribution of FM-related spectral weight involves significantly different energy scales than those observed in the non-magnetic samples. In the polycrystalline LaCoO₃ and the compressively strained LaCoO₃/LaAlO₃ film, the majority of the spectral weight redistribution at low energies occurs between 0.2 and 1.7-1.9 eV, see Figs. 3(d) and (e). In contrast, in the FM LaCoO₃/LSAT film, the low-energy wing spans between 0.2-3.3 eV with the maximum in the interval between 2 and 2.8 eV where the conductivity changes in the non-magnetic samples are only minor. We think this sizable difference reflects the FM interaction of the HS states that is absent in the non-magnetic samples. We believe that this sizable change in the involved energy scale is potentially important and should be explained by a theory aiming at a full understanding of the strained-induced FM state in LaCoO₃.

Figure 3(l) displays the temperature dependence of the effective concentration of charge carriers $N_{\text{eff}}(E_g, E_M)$ in the interval of the low-energy “wing”. The amount of the spectral weight redistributed due to the formation of the FM state, $N_{\text{eff}}^{\text{FM}}$, is estimated (as shown by the arrow) as the difference of $N_{\text{eff}}(E_g, E_M)$ between the value at 7 K

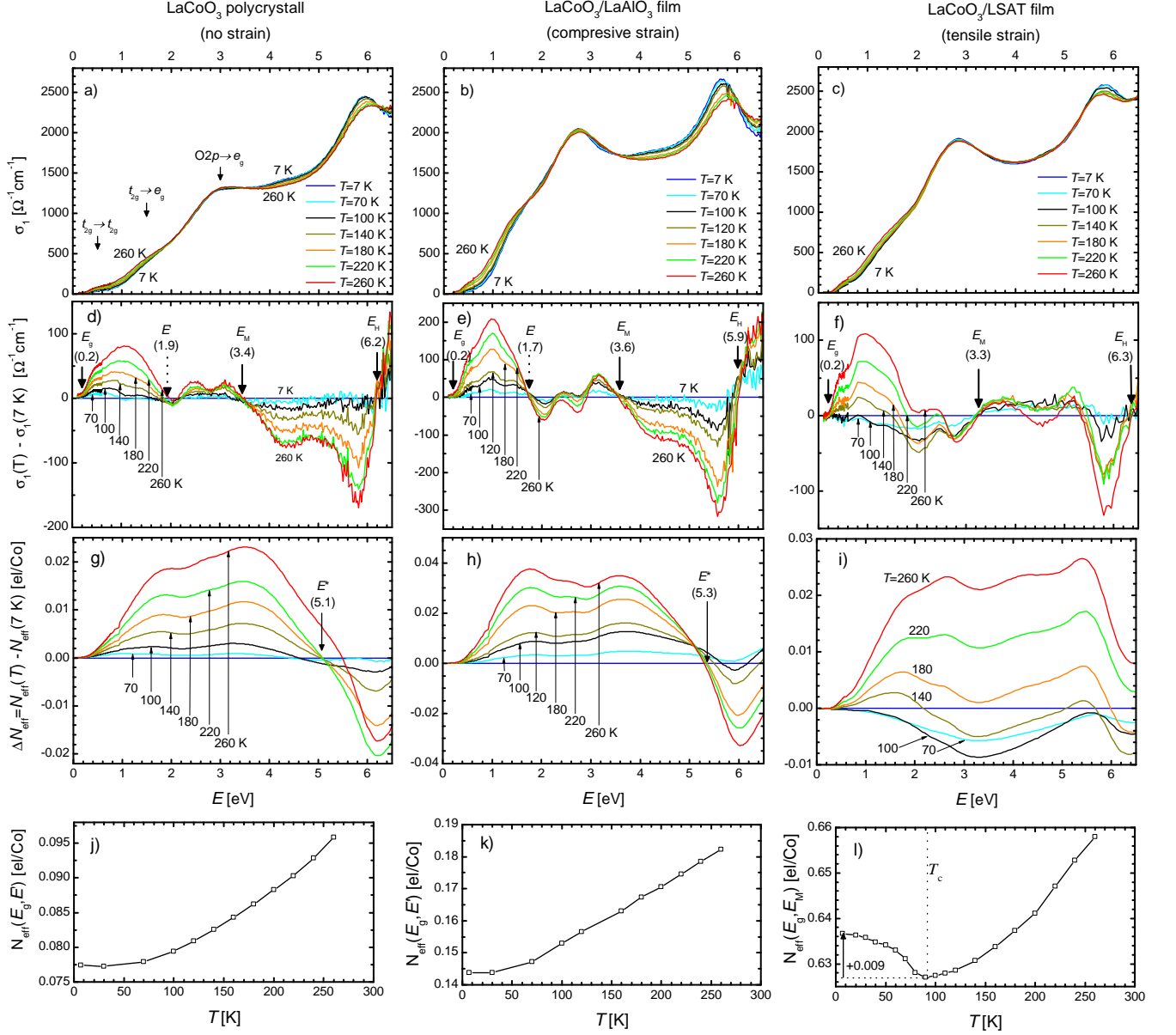


FIG. 3. An overview of the optical data. The left, middle, and right columns correspond to the unstrained LaCoO_3 polycrystall, compressively strained $\text{LaCoO}_3/\text{LaAlO}_3$ thin film, and tensile strained $\text{LaCoO}_3/\text{LSAT}$ film, respectively. The top row (a)-(c): the real part of the optical conductivity $\sigma_1(E, T)$ as a function of the energy E and temperature T . The second row (d)-(f): $\sigma_1(T) - \sigma_1(7 \text{ K})$. The third row (g)-(i): $\Delta N_{\text{eff}}(E) = N_{\text{eff}}(0.1 \text{ eV}, E, T) - N_{\text{eff}}(0.1 \text{ eV}, E, T = 7 \text{ K})$, see Eq.(1), as a function of the high energy cutoff E . Panels (j) and (k) show the temperature dependence of $N_{\text{eff}}(E_g, E')$ and panel (l) shows $N_{\text{eff}}(E_g, E_M)$.

and right above the T_c and amounts to $N_{\text{eff}}^{\text{FM}} = +0.009$ elementary charge per Co ion. This estimate neglects the temperature dependence of $N_{\text{eff}}(E_g, E_M)$ due to processes unrelated to FM ordering. We believe that they are low, and if taken into account, they would slightly increase the obtained value of $N_{\text{eff}}^{\text{FM}}$. Providing the low-energy spectral weight $N_{\text{eff}}(E_g, E_M)$ is proportional to the population of HS states, its temperature variation shown in Fig. 3(l) can be qualitatively understood in the framework of the biexciton model of the strained-induced

FM state [10]. Above T_c , the concentration of HS states is expected to decrease with decreasing temperature as the thermally populated HS states relax into LS states. Below T_c , HS states get stabilized by the FM interaction, and thus, their concentration starts to increase with decreasing temperature.

The value of $N_{\text{eff}}^{\text{FM}}$ can be estimated as well from $\Delta N_{\text{eff}}(E)$ shown in Fig. 3(i) where for $T = 100 \text{ K}$, the value of $\Delta N_{\text{eff}}(E)$ near 3.3 eV yields the value of -0.009 . Additionally, $\Delta N_{\text{eff}}(T = 100 \text{ K})$ amounts to -0.001 at

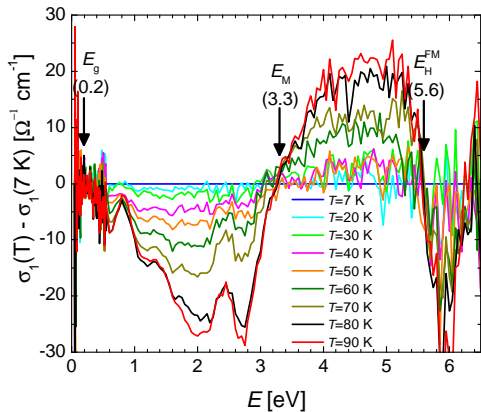


FIG. 4. The real part of the optical conductivity of the ferromagnetic LaCoO₃/LSAT film with respect to 7 K, $\sigma_1(E, T) - \sigma_1(E, 7 \text{ K})$, below and near $T_c = 82 \text{ K}$.

$E_H^{FM} = 5.6 \text{ eV}$ and thus almost reaches zero depicting that within the accuracy of about 10%, the spectral weight of the high-energy wing compensates for the low-energy wing, and thus the spectral weight below T_c is essentially conserved below $E_H^{FM} = 5.6 \text{ eV}$. In this context, it is interesting to note that at 260 K, $\Delta N_{\text{eff}}(E)$ does not exhibit any zero crossing in the measured range, and at 6.5 eV amounts to a sizable value of 0.008. This demonstrates that in the tensile strained LaCoO₃, the spectral weight redistribution at temperatures above T_c involves transitions at energies above those occurring in the paramagnetic phase of the unstrained polycrystalline LaCoO₃, see Fig. 3(g), and reaches energies beyond our measurement limit of 6.5 eV.

Note that the direction (or sign) of the FM-induced spectral weight redistribution is the same as in the double exchange FM state in doped cobaltites [5], where the FM order is driven by the reduction in the kinetic energy caused by the delocalization of the conducting electrons. Obviously, in LaCoO₃, the DC conductivity is absent; however, this does not exclude that the ferromagnetic state is driven by a decrease of the kinetic energy on a finite scale. This motivated us to quantify the reduction of the kinetic energy ΔK corresponding to the FM-related redistribution of the spectral weight, $N_{\text{eff}}^{\text{FM}}$. As a rough estimate, we use the same formula as in Ref. [5], $\Delta K = -\frac{3\hbar^2}{a_0^2 m_0} N_{\text{eff}}^{\text{FM}}$, where ΔK is the change of kinetic energy, \hbar is the reduced Planck's constant, and a_0 is the lattice constant. This relation was derived for the intraband kinetic energy [33]. Nevertheless, we use it here merely as a phenomenological estimate of the kinetic energy reduction, even in the present case of interband transitions. Using the value $N_{\text{eff}}^{\text{FM}} = +0.009$ we obtain $\Delta K = -13 \text{ meV}$. Providing the latter estimate is correct, the change of kinetic energy is about two times the thermal energy at T_c , $|\Delta K/k_B T_c| \sim 2$, which shows that the reduction of the kinetic energy is an important quantity that may play a leading role in the mechanism of ferro-

magnetism in strained LaCoO₃. Note that since the penetration depth in LaCoO₃ in the whole measured range is larger than the thickness of the films (about 22 nm), our optical measurements represent an average response of the films. Our findings, therefore, show that the strain-induced FM state is pronounced and probably occurs in the whole or large portion of the film. Note additionally that the value of $\Delta K/k_B T_c \sim 2$ is essentially the same as the value found for the double-exchange ferromagnetism in doped cobaltites [5], again depicting the importance of the magnitude of the FM-related spectral weight redistribution observed in LaCoO₃/LSAT thin film.

IV. SUMMARY

Using spectroscopic ellipsometry, we have measured the optical conductivity of LaCoO₃ with various degrees of strain. The optical response of the compressively strained LaCoO₃ film grown on LaAlO₃ substrate is qualitatively similar to that of the unstrained LaCoO₃ polycrystalline sample. They both exhibit, with increasing temperature, a transfer of spectral weight from high energies between about 3.5 and 6 eV to lower energies, mostly between 0.2 and 1.9 eV. This redistribution of spectral weight is most likely related to the thermal excitation of the high-spin states.

The optical response of the ferromagnetic tensile strained LaCoO₃/LSAT film exhibits clear signatures due to the ferromagnetic state. Below the Curie temperature $T_c = 82 \text{ K}$, the spectral weight is transferred with the increasing temperature from low energies between 0.2 and 3.3 eV to high energies between 3.3 and 5.6 eV. The sizable spectral range difference of the spectral weight redistribution at low energies with respect to the relaxed LaCoO₃ (3.3 eV instead of 1.9 eV) most likely reflects the ferromagnetic interaction of the high-spin biexcitons and may be of interest for theoretical predictions. The temperature dependence of the low-energy spectral weight between 0.2 and 3.3 eV can be understood in the framework of the high-spin biexciton model as being due to the variation of the concentration of high-spin states that with lowering temperature are stabilized below T_c . The amount of spectral weight redistributed due to the formation of the ferromagnetic state is sizable and corresponds to 0.009 elementary charge per Co ion. We estimate that it is equivalent to the saved kinetic energy of $\Delta K = 13 \text{ meV}$. The ratio of ΔK with respect to $k_B T_c$ is about 2, which shows that the reduction of kinetic energy is an important quantity that may be a leading factor in the formation of the ferromagnetic state.

ACKNOWLEDGMENTS

We thank O. Caha, J. Chaloupka, A. Hariki, J. Kuneš, D. Munzar, and A. Sotnikov for the fruitful discussions. We acknowledge the usage of data measured by P. Friš.

We acknowledge the financial support by the project Quantum materials for applications in sustainable technologies, CZ.02.01.01/00/22_008/0004572, the MEYS of the Czech Republic under the project CEITEC 2020 (LQ1601), by the Czech Science Foundation (GACR)

under Project No. GA20-10377S and CzechNanoLab project LM2023051 funded by MEYS CR for the financial support of the measurements/sample fabrication at CEITEC Nano Research Infrastructure.

-
- [1] Y. Tokura, Y. Okimoto, S. Yamaguchi, H. Taniguchi, T. Kimura, and H. Takagi, *Phys. Rev. B* **58**, R1699 (1998).
- [2] D. W. Jeong, W. S. Choi, S. Okamoto, J.-Y. Kim, K. W. Kim, S. J. Moon, D.-Y. Cho, H. N. Lee, and T. W. Noh, *Sci. Rep.* **4**, 06124 (2014).
- [3] D. Fuchs, C. Pinta, T. Schwarz, P. Schweiss, P. Nagel, S. Schuppler, R. Schneider, M. Merz, G. Roth, and H. von Löhneysen, *Phys. Rev. B* **75**, 144402 (2007).
- [4] D. Fuchs, M. Merz, P. Nagel, R. Schneider, S. Schuppler, and H. von Löhneysen, *Phys. Rev. Lett.* **111**, 257203 (2013).
- [5] P. Friš, D. Munzar, O. Caha, and A. Dubroka, *Phys. Rev. B* **97**, 045137 (2018).
- [6] J. Fujioka, Y. Yamasaki, H. Nakao, R. Kumai, Y. Murakami, M. Nakamura, M. Kawasaki, and Y. Tokura, *Phys. Rev. Lett.* **111**, 027206 (2013).
- [7] N. Biskup, J. Salafranca, V. Mehta, M. P. Oxley, Y. Suzuki, S. J. Pennycook, S. T. Pantelides, and M. Varela, *Phys. Rev. Lett.* **112**, 087202 (2014).
- [8] V. V. Mehta, N. Biskup, C. Jenkins, E. Arenholz, M. Varela, and Y. Suzuki, *Phys. Rev. B* **91**, 144418 (2015).
- [9] Q. Feng, D. Meng, H. Zhou, G. Liang, Z. Cui, H. Huang, J. Wang, J. Guo, C. Ma, X. Zhai, Q. Lu, and Y. Lu, *Phys. Rev. Mater.* **3**, 074406 (2019).
- [10] A. Sotnikov, K.-H. Ahn, and J. Kuneš, *SciPost Phys.* **8**, 082 (2020).
- [11] F. M. F. de Groot, J. C. Fuggle, B. T. Thole, and G. A. Sawatzky, *Phys. Rev. B* **42**, 5459 (1990).
- [12] M. A. Korotin, S. Y. Ezhov, I. V. Solovyev, V. I. Anisimov, D. I. Khomskii, and G. A. Sawatzky, *Phys. Rev. B* **54**, 5309 (1996).
- [13] C. Zobel, M. Kriener, D. Bruns, J. Baier, M. Gruninger, T. Lorenz, P. Reutler, and A. Revcolevschi, *Phys. Rev. B* **66**, 020402(R) (2002).
- [14] A. Ishikawa, J. Nohara, and S. Sugai, *Phys. Rev. Lett.* **93**, 136401 (2004).
- [15] J. Q. Yan, J. S. Zhou, and J. B. Goodenough, *Phys. Rev. B* **69**, 134409 (2004).
- [16] M. W. Haverkort, Z. Hu, J. C. Cezar, T. Burnus, H. Hartmann, M. Reuther, C. Zobel, T. Lorenz, A. Tanaka, N. B. Brookes, H. H. Hsieh, H. J. Lin, C. T. Chen, and L. H. Tjeng, *Phys. Rev. Lett.* **97**, 176405 (2006).
- [17] Z. Ropka and R. J. Radwanski, *Phys. Rev. B* **67**, 172401 (2003).
- [18] A. Podlesnyak, S. Streule, J. Mesot, M. Medarde, E. Pomjakushina, K. Conder, A. Tanaka, M. W. Haverkort, and D. I. Khomskii, *Phys. Rev. Lett.* **97**, 247208 (2006).
- [19] M. Merz, P. Nagel, C. Pinta, A. Samartsev, H. v Löhneysen, M. Wissinger, S. Uebe, A. Assmann, D. Fuchs, and S. Schuppler, *Phys. Rev. B* **82**, 174416 (2010).
- [20] V. Krápek, P. Novák, J. Kuneš, D. Novoselov, D. M. Korotin, and V. I. Anisimov, *Phys. Rev. B* **86**, 195104 (2012).
- [21] A. Sotnikov and J. Kunes, *Sci. Rep.* **6**, 30510 (2016).
- [22] R.-P. Wang, A. Hariki, A. Sotnikov, F. Frati, J. Okamoto, H.-Y. Huang, A. Singh, D.-J. Huang, K. Tomiyasu, C.-H. Du, J. Kuneš, and F. M. F. de Groot, *Phys. Rev. B* **98**, 035149 (2018).
- [23] A. Hariki, R.-P. Wang, A. Sotnikov, K. Tomiyasu, D. Betto, N. B. Brookes, Y. Uemura, M. Ghiasi, F. M. F. de Groot, and J. Kuneš, *Phys. Rev. B* **101**, 245162 (2020).
- [24] D. Fuchs, E. Arac, C. Pinta, S. Schuppler, R. Schneider, and H. von Löhneysen, *Phys. Rev. B* **77**, 014434 (2008).
- [25] A. Herklotz, A. D. Rata, L. Schultz, and K. Doerr, *Phys. Rev. B* **79**, 092409 (2009).
- [26] V. V. Mehta, M. Liberati, F. J. Wong, R. V. Chopdekar, E. Arenholz, and Y. Suzuki, *J. Appl. Phys.* **105**, 07E503 (2009).
- [27] A. D. Rata, A. Herklotz, L. Schultz, and K. Doerr, *Eur. Phys. J. B* **76**, 215 (2010).
- [28] W. S. Choi, J.-H. Kwon, H. Jeon, J. E. Hamann-Borrero, A. Radi, S. Macke, R. Sutarto, F. He, G. A. Sawatzky, V. Hinkov, M. Kim, and H. N. Lee, *Nano Lett.* **12**, 4966 (2012).
- [29] D. N. Basov, R. D. Averitt, D. van der Marel, M. Dressel, and K. Haule, *Rev. Mod. Phys.* **83**, 471 (2011).
- [30] By Alineason Materials Technology GmbH, Germany.
- [31] H. G. Tompkins and E. A. Irene, eds., *Handbook of ellipsometry* (William Andrew, Inc., 2005).
- [32] M. Zahradník, M. Kiaba, S. Espinoza, M. Rebarz, J. Andreasson, O. Caha, F. Abadizaman, D. Munzar, and A. Dubroka, *Phys. Rev. B* **105**, 235113 (2022).
- [33] D. N. Basov and T. Timusk, *Rev. Mod. Phys.* **77**, 721 (2005).